Topologically stable gapped state in a layered superconductor

2014 EPL 105 31002

(http://iopscience.iop.org/0295-5075/105/3/31002)

A Letters Journal Exploring the Frontiers of Physics

February 2014

EPL, **105** (2014) 31002
doi: 10.1209/0295-5075/105/31002

www.epljournal.org

Topologically stable gapped state in a layered superconductor

Marco Cariglia[1], Alfredo A. Vargas-Paredes[2] and Mauro M. Doria[2]

[1] *Departamento de Física, Universidade Federal de Ouro Preto - 35400-000 Ouro Preto Minas Gerais, Brazil*
[2] *Departamento de Física dos Sólidos, Universidade Federal do Rio de Janeiro 21941-972 Rio de Janeiro, Brazil*

received 14 October 2013; accepted in final form 27 January 2014
published online 20 February 2014

PACS 12.39.Dc – Skyrmions
PACS 74.20.De – Phenomenological theories (two-fluid, Ginzburg-Landau, etc.)
PACS 74.72.Kf – Pseudogap regime

Abstract – We show that a layered superconductor, described by a two-component order parameter, has a gapped state above the ground state, topologically protected from decay, containing flow and counterflow in the absence of an applied magnetic field. This state is made of skyrmions, breaks time reversal symmetry and produces a weak local magnetic field. We estimate the density of carriers that condense into the pseudogap of the cuprate superconductors based on the assumption that the pseudogap is a skyrmion state.

Introduction. – An important concept in condensed matter physics is that of an order parameter (OP), introduced by Lev Landau in the last century to describe the transition to the superconducting state. Interestingly, one of Landau's first proposals of an order parameter was the supercurrent, also suggested to exist in the microscopic superconducting ground state of Felix Bloch [1]. These ideas were soon dismissed since a spontaneous circulating supercurrent increases the kinetic energy. In this letter we find an excited but stable state with these spontaneously circulating supercurrents, containing flow and counterflow in the layers, even without the presence of an external magnetic field. This is a skyrmion state found to exist above the homogeneous state in a layered superconductor, described by a two-component OP. The decay of the skyrmion state into other configurations of lower free energy is prevented by its topological stability, which gives rise to an energy gap. The skyrmion state breaks the time reversal symmetry and produces a very weak magnetic field inside the superconductor due to the supercurrents. The gap above the ground state, the topological stability and the unusual magnetic order that breaks the time reversal symmetry found here leads us to suggest that the pseudogap of the layered superconductors is indeed a skyrmion state.

Cuprate superconductors. – The temperature-*vs.*-doping diagram of the cuprate superconductors has three basic common features: i) an antiferromagnetic Mott insulator state based on Cu^{2+} spins at zero doping that rapidly disappears by increasing the doping; ii) a superconducting state under a dome-shaped curve that defines the critical temperature T_c, whose maximum, T_c^{max}, defines the underdoped, optimally doped, and overdoped states, respectively; and iii) a pseudogap state that emerges in the underdoped regime at a temperature T^*, claimed to be a phase transition line when plotted *vs.* doping [2]. It decreases with increasing doping level, and, at a particular doping [3], the pseudogap and the superconducting transition coincide, $T^* = T_c$ in the slightly overdoped regime.

The pseudogap state [4] breaks the time-reversal symmetry [2,5,6], as dichroism has been observed below T^* [6]. A state described by an OP with broken time reversal symmetry must have an accompanying magnetic order [7] and, for this reason, there has been an intense search for this accompanying magnetic order associated to the pseudogap. Proposals have been made to explain it, such as by Varma [8], based on microscopic orbital currents. Indeed polarized neutron diffraction experiments [9,10] indicate a magnetic order below the pseudogap, but NMR/NQR [11,12] and μSR [13,14] experiments set a very restrictive limit to *the maximum magnetic field* inside the superconductor, hereafter called h_{max}, which cannot be larger than $h_{max} \sim 0.1$ to 0.01 G. We show here that the skyrmion state breaks the time reversal symmetry and links the pseudogap to the weak internal magnetic field h_{max}.

Since the discovery of stripe order in the cuprates, charge, magnetism and superconductivity are believed to coexist in geometrical periodic arrangements [15]. The pseudogap also breaks the translational symmetry since a tetragonal lattice, the so-called checkerboard pattern (CB), is found there. The CB is commonly associated to a charge density wave [16], has the size of four times the crystallographic unit cell and was firstly discovered by scanning tunneling microscopy inside the vortex cores [17] of $Bi_2Sr_2CaCu_2O_{8+x}$. Later the CB was also found in the absence of a magnetic field in a slightly underdoped version of this compound above the superconducting transition temperature [18]. The CB is not necessarily commensurate with the crystallographic structure [19]. It has been observed by distinct experimental techniques, such as X-ray scattering, used to report an intrinsically modulated kinetic lattice four times the crystallographic unit cell [20] in the optimally doped $YBa_2Cu_3O_{6.92}$ compound, above and below T_c. The possibility of describing the CB through an OP has been considered by Rosen *et al.* [21].

The tetragonal symmetry. – We claim that a two-component OP Ginzburg-Landau theory can describe the superconducting and the pseudogap states of the layered compounds, above and below the critical temperatures T_c and T^*, in the neighborhood $T \approx T_c \approx T^*$ where a power expansion of the free energy in terms of an OP is attainable. Here we suggest that the breaking of both time and translational invariance symmetries are consequences of a skyrmion state, whose intrinsically circulating currents in the layers, naturally produce a charge density wave, since the divergence of the superficial current does not necessarily vanish within a layer. The detailed description of this charge density wave associated to the skyrmion lattice will be given elsewhere. Here we obtain the skyrmion solution of the two-component OP theory. We consider the particular temperature $T = T_c = T^*$, because at this temperature there are no free parameters, as the condensate energy is nearly zero, since it becomes of fourth-order power in the OP. Therefore at this temperature there should exist material independent universal properties of the layered superconductors. The free energy reduces to a sum of the kinetic and of the magnetic energies, which are both positive and the homogeneous state, which has the OP and the local magnetic field equal to zero, has the lowest free energy. Nevertheless above it lives the skyrmion state, an inhomogeneous state with non-vanishing OP and non-vanishing local magnetic field, topologically protected from decay into the homogeneous ground state. The circulating supercurrents in the layers associated to the skyrmion state for d- and s-wave cases can be seen in fig. 1 inside the cell.

We show here that the kinetic energy of the skyrmion state yields a gap, which we claim to be the pseudogap itself. The magnetic energy is residual in comparison to the kinetic energy since h_{max} must fall below the experimental threshold described before. Nevertheless the

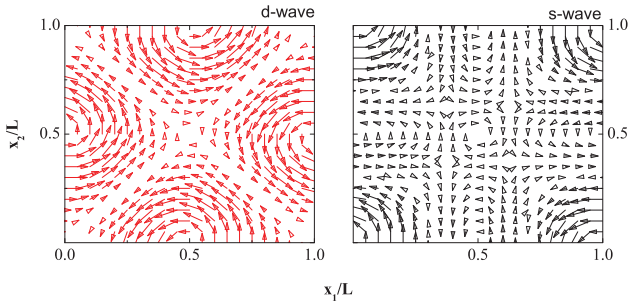

Fig. 1: (Color online) The superficial current $\vec{J}_s$ is shown for d and s waves for a square unit cell. The two d-wave skyrmions are centered in the middle of the sides and the single s-wave skyrmion is at the corner.

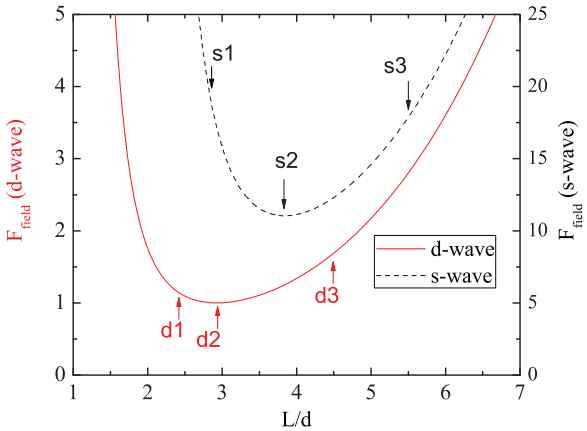

Fig. 2: (Color online) The magnetic energy between layers *vs.* L/d is shown here. Three L/d ratios are shown for d-wave, 2.42 (d1), 2.94 (d2) and 4.49 (d3), and also for s-wave, 2.86 (s1), 3.83 (s2), and 5.50 (s3). The d2 and s2 points are the minimum of d- and s-wave curves, respectively. The curves are normalized to the minimum of the d-wave magnetic energy.

skyrmion lattice stores magnetic energy between layers because of the circulating supercurrents. This magnetic energy reaches a minimum with respect to the ratio L/d, where d is the interlayer distance, as shown in fig. 2 for d- and s-wave symmetry, respectively. Interestingly below a certain ratio, $L/d \approx 2.2$, the skyrmions disappear for both d- and s-wave symmetries. Considering a crystallographic cell with size $a \approx 0.39\,\text{nm}$, and $d \approx 1.17\,\text{nm}$, such as in $YBa_2Cu_3O_{6.92}$, this lowest bound becomes $L/a \approx 6.6$. Notice that in case of d-wave the unit cell, as shown in fig. 1, contains two skyrmions. Hence a smaller unit cell with a single skyrmion has a size $L' = L/\sqrt{2}$, and in this case, $L'/a \approx 4.7$, thus very close to the commonly observed CB cell of $L = 4a$, such as in the optimally doped $YBa_2Cu_3O_{6.92}$ [20]. The fact that the checkerboard size does not fall exactly in the magnetic energy minimum of fig. 2 must be a consequence of some discarded residual interaction, such as the fourth-order OP correction present in the condensate energy. In summary, the theoretically predicted skyrmion lattice falls within the range of the

observed CB and so the later can be expected to be a consequence of the former. The fact that the temperature $T = T_c = T^*$ is supposedly near to $T = T_c^{max}$, allows us to estimate the number of carriers in the pseudogap for the optimal doping.

The number of carriers in the pseudogap. – The interpretation of the pseudogap as a skyrmion state leads to the estimate that the number of carriers that condense in the pseudogap of the cuprate superconductors near optimal doping is 0.01% of the Cooper pair density. Let the number of carriers that condense in the pseudogap be n_{pg}. Our starting point is the large wavelength limit of the kinetic energy density, F_k, (eq. (14)) of the skyrmion state, responsible for the pseudogap density. For the single-layer cuprate we obtain that $F_k \sim 0.1 h_{max}\,\mathrm{meV}\cdot\mathrm{nm}^{-3}$, where h_{max} is given in gauss. Taking that $h_{max} \sim 0.01\,\mathrm{G}$, thus below the experimental threshold, the pseudogap density becomes $F_k \sim 10^{-3}\,\mathrm{meV}\cdot\mathrm{nm}^{-3}$. From this pseudogap density follows the density of carriers under the extra assumption that near optimal doping the pseudogap and the superconducting gap of the cuprates have similar values. According to the BCS the superconducting state lies below the normal state by the gap density of $F_{gap} = 2\Delta n_g$, where 2Δ is the energy required to break a single Cooper pair and n_g represents the density of available Cooper pairs, namely $n_g = 0.187\Delta n/E_F$, n and E_F being the electronic density and the Fermi energy, respectively. Then one obtains that the gap density for metals is $F_{gap} \sim 10^{-4}\,\mathrm{meV}\cdot\mathrm{nm}^{-3}$ since $n \sim 0.1\,\mathrm{nm}^{-3}$, $\Delta/E_F \sim 10^{-4}$ and $2\Delta \sim 1.0\,\mathrm{meV}$. A similar estimate for the cuprates gives that the gap density is $F_{gap} \sim 10\,\mathrm{meV}\cdot\mathrm{nm}^{-3}$, considering that the gap is ten times larger than that of metals, $2\Delta \sim 10\,\mathrm{meV}$, and $n_g \sim 1.0\,\mathrm{nm}^{-3}$, since there are a few Cooper pairs [22] occupying the coherence length volume, $\xi_{ab}^2\xi_c$, where $\xi_{ab} \sim 1.5\,\mathrm{nm}$, $\xi_c \sim 0.3\,\mathrm{nm}$. Assuming that the skyrmion pseudogap density is the product of a pseudogap times a density, $F_k \to 2\Delta_{pg} n_{pg}$, and that, $2\Delta_{pg} \sim 10\,\mathrm{meV}$, we conclude that $n_{pg} \sim 10^{-4}\,\mathrm{nm}^{-3}$. Therefore the ratio between the pseudogap and gap carrier densities is $n_{pg}/n_g \sim 10^{-4}$.

First-order equations. – We derive the OP and the local magnetic field associated to the skyrmion state from the *first-order equations* (FOE) instead of the second-order variational equations. Interestingly Abrikosov [23], used the FOE to discover the vortex lattice instead of the second-order Ginzburg-Landau (GL) variational equations. The GL free energy only sorts among the possible vortex lattice the one with minimal energy. Later the FOE were rediscovered by Bogomolny [24] in the context of string theory and shown to solve exactly the GL second-order equations for a particular value of the coupling constant. The Seiberg-Witten equations, which also describe topological excitations, namely four-dimensional monopoles [25], are FOE that belong to the same family of the Abrikosov-Bogomolny (AB) equations. In this family, the FOE determine the OP and the vector potential associated to topological excitations. In this letter we obtain the topological solutions (skyrmions) associated to another set of equations that belong to this family that lives in the three-dimensional Euclidean space [26,27]. The existence of topological solutions for the two-component GL theory was pointed out long ago [28], through a mapping into a nonlinear $O(3)$ sigma model.

The skyrmion state. – In his original work T. Skyrme made protons and neutrons stable by association to a topologically non-trivial solution of the sigma model [29, 30], the skyrmion, that represents a configuration with particle-like properties. Skyrmions are found in many condensed matter systems with an inner structure constructed over a physical OP. Skyrmions were reported in the quantized Hall effect [31], Bose-Einstein condensates [32] and superfluid^{3}He-A [33]. In the antiferromagnet $La_2Cu_{1-x}Li_xO_4$ [34] the CuO_2 layers are modified by Li atoms, which are dopants that frustrate the original Neel state, leading to a magnetic state made of skyrmions. Recently skyrmions were found to form a crystalline order [35] in the helimagnet MnSi [36] and also in the doped semiconductor $Fe_{1-x}Co_xSi$ [37].

The present skyrmion state stems from the superficial supercurrent $\vec{J}_s$ circulating in the layers that generates a spatial magnetic field $\vec{h}$ [38]. As shown in fig. 1, there are two cores of $\vec{J}_s$ for d-wave (red), with centers in the middle of the unit cell sides, while for s-wave (black) there is only one core centered at the corners of the unit cell. In both cases, there is no net circulation in the unit cell, and yet there is a single sense of intense circulation set by the cores. As seen from above a layer, *e.g.* the plane of fig. 1, the $\vec{h}$ stream lines sink into these cores to reemerge from below, and pierce the unit cell a second time, forming closed loops. The field stream lines are densely concentrated in the cores. There are some stream lines that fully cross the stack of layers, in the opposite direction relative to the sinking ones, never to come back again, like in an infinitely extended solenoid. The skyrmion cores are small, concentrated pockets of opposite field with 9.4% and 5.3% of the total cell area, for d- and s-wave, respectively.

The skyrmion's topological charge is obtained by integration over a single layer, at $x_3 = 0$ for $\hat{h} = \vec{h}/|\vec{h}|$.

$$Q = \frac{1}{4\pi}\int_{L^2,\,x_3=0^+}\left(\frac{\partial\hat{h}}{\partial x_1}\times\frac{\partial\hat{h}}{\partial x_2}\right)\cdot\hat{h}\;\mathrm{d}^2x, \qquad (1)$$

and one obtains that $Q = -2$ and -1 for the d- and s-wave states, respectively, in agreement with the plotted solutions of fig. 1. Clearly the time reversal symmetry, $(\vec{h} \to -\vec{h})$, is broken by the skyrmions.

The theory. – Two-component OP theories are being considered to describe properties of the high-temperature layered superconductors [39] and only a multi-component OP theory can yield a time reversal broken state [40,41]. We assume that the free energy density of a layered superconductor is a sum of the kinetic, field and condensate

energy densities [26,27], $F = F_k + F_f + F_c$,

$$F_k = \left\langle \frac{|\vec{D}\Psi|^2}{2m} \right\rangle, \quad \Psi = \begin{pmatrix} \psi_u \\ \psi_d \end{pmatrix}, \quad \text{and } F_f = \left\langle \frac{\vec{h}^2}{8\pi} \right\rangle, \tag{2}$$

where $\langle \cdots \rangle \equiv \int \left(\mathrm{d}^3x/V\right)(\cdots)$ and V is the bulk volume. There is minimal coupling, $\vec{D} = (\hbar/i)\vec{\nabla} - (q/c)\vec{A}$, and the local magnetic field is $\vec{h} = \vec{\nabla} \times \vec{A}$. The most general condensate energy density is $F_c = \langle -\alpha_0 \Psi^\dagger\Psi - \vec{\alpha}\cdot\Psi^\dagger\vec{\sigma}\Psi + \beta_{a,b,c,d}\,\psi_a^*\psi_b^*\psi_c\psi_d/2\rangle$, where indices a, b, c, d run over u and d, and $\vec{\sigma}$ are the Pauli matrices. For $T = T^* = T_c$, the free energy density becomes $F = F_k + F_f$ [26,27] since F_c is negligible by fluctuation theory [42] arguments. The order parameter is so small that its fourth-order power terms can be abandoned in face of the second-order power ones: $F_c \approx -(\alpha_0 + \alpha_3)\langle|\psi_u|^2\rangle - (\alpha_0 - \alpha_3)\langle|\psi_d|^2\rangle - \vec{\alpha}_\parallel \cdot \langle\Psi^\dagger\vec{\sigma}_\parallel\Psi\rangle$, where the parallel components are along the layers by choice of coordinate system. The temperature $T = T^* = T_c$ corresponds exactly to $\alpha_0 + \alpha_3 = 0$ and $\alpha_0 - \alpha_3 = 0$. Then $F_c \approx -\vec{\alpha}_\parallel \cdot \langle\Psi^\dagger\vec{\sigma}_\parallel\Psi\rangle$ and we shall see below that for the skyrmion state $\langle\Psi^\dagger\vec{\sigma}_\parallel\Psi\rangle = 0$, which leads to $F_c \approx 0$.

The second-order variational equations must be solved for a set of equally spaced superconducting layers such that two-dimensional layers carry a $\vec{J}_s$, and away from them the condensate evanesces exponentially in a metallic environment. We find this solution by means of the FOE method, which solves Ampère's law exactly, $\vec{\nabla}\times\vec{h} = 4\pi\vec{J}/c$, $\vec{J} = (q/2m)\big(\Psi^\dagger\vec{D}\Psi + \text{c.c.}\big)$, and the Ginzburg-Landau equation, $\vec{D}^2\Psi = 0$ approximately, meaning that, instead, we solve exactly the so-called integrated equation, $\langle\Psi^\dagger\vec{D}^2\Psi\rangle = 0$, which can also be expressed as $\langle|\vec{D}\Psi|^2 - (\hbar/2)\vec{\nabla}^2|\Psi|^2\rangle = 0$. The FOE method relies on the following identity, which allows for a twofold view of the kinetic energy [27]:

$$\frac{1}{2m}\left|\vec{D}\Psi\right|^2 = \frac{1}{2m}\left|\vec{\sigma}\cdot\vec{D}\Psi\right|^2 + \frac{\hbar q}{2mc}\vec{h}\cdot\Psi^\dagger\vec{\sigma}\Psi - \frac{\hbar}{4m}\vec{\nabla}\left[\Psi^\dagger\left(\vec{\sigma}\times\vec{D}\right)\Psi + \text{c.c.}\right]. \tag{3}$$

From it an equivalent, but distinct, formulation of the current density is obtained,

$$\vec{J} = \frac{q}{2m}\left[\Psi^\dagger\vec{\sigma}\left(\vec{\sigma}\cdot\vec{D}\Psi\right) + \text{c.c.}\right] - \frac{\hbar q}{2m}\vec{\nabla}\times\left(\Psi^\dagger\vec{\sigma}\Psi\right). \tag{4}$$

Imposing that the order parameter satisfies

$$\vec{\sigma}\cdot\vec{D}\,\Psi = 0, \tag{5}$$

leads to the exact determination of the local field from Ampère's law,

$$\vec{h} = \vec{C} - 4\pi\mu_B\Psi^\dagger\vec{\sigma}\Psi, \tag{6}$$

where $\mu_B = \hbar q/2mc$ is Bohr's magneton. Thus for fields that satisfy the FOE, eq. (3) becomes

$$\frac{1}{2m}\left|\vec{D}\Psi\right|^2 = \mu_B\left(\vec{C} - 4\pi\mu_B\Psi^\dagger\vec{\sigma}\Psi\right)\cdot\Psi^\dagger\vec{\sigma}\Psi + \frac{\hbar^2}{4m}\nabla^2\left(\Psi^\dagger\Psi\right) \tag{7}$$

Introducing eq. (7) into the integrated equation gives that $\langle(\vec{C} - 4\pi\mu_B\Psi^\dagger\vec{\sigma}\Psi)\cdot\Psi^\dagger\vec{\sigma}\Psi\rangle = 0$, which is exactly solved for the following choice of integration constant:

$$\vec{C} = 4\pi\mu_B\langle\Psi^\dagger\vec{\sigma}\Psi\rangle\frac{\langle\left(\Psi^\dagger\vec{\sigma}\Psi\right)^2\rangle}{\langle\Psi^\dagger\vec{\sigma}\Psi\rangle^2}. \tag{8}$$

Thus one obtains that,

$$F_k = \frac{\hbar^2}{4m}\langle\vec{\nabla}^2\left(\Psi^\dagger\Psi\right)\rangle, \text{ and} \tag{9}$$

$$F_f = 2\pi\mu_B^2\langle\left(\Psi^\dagger\vec{\sigma}\Psi\right)^2\rangle\left[\frac{\langle\left(\Psi^\dagger\vec{\sigma}\Psi\right)^2\rangle}{\langle\Psi^\dagger\vec{\sigma}\Psi\rangle^2} - 1\right]. \tag{10}$$

Equations (5) and (6) are nonlinear and must be solved iteratively. The first one determines Ψ while the second one, $\vec{h}$. We solve them in the lowest-order approximation, that is, firstly Ψ is obtained from eq. (5) in the absence of $\vec{h}$, and, next, $\vec{h}$ is determined from eq. (6), using the known OP solution. The success of this lowest approximation relies on the fact that $\vec{h}$ must be very weak, such that no further iterations of the FOE are needed. For the case of a single layer, the solution of $\vec{\sigma}\cdot\vec{\nabla}\Psi = 0$ is, for $x_3 \neq 0$,

$$\Psi = \sum_{\vec{k}\neq 0} c_{\vec{k}}\, e^{-k|x_3|}e^{i\vec{k}\cdot\vec{x}}\begin{pmatrix} 1 \\ -i\frac{k_+}{k}\frac{x_3}{|x_3|} \end{pmatrix}, \tag{11}$$

where $k_\pm = k_1 \pm ik_2$. The space-time symmetries are broken, namely, the reflection symmetry, $x_3 \to -x_3$, and also the time reversal symmetry, $k_+ \to k_-$. Although these features reflect our particular choice of a basis, they are intrinsic to the solution and cannot be removed from it. Notice that the density $\Psi^\dagger\Psi$ and $\Psi^\dagger\sigma_3\Psi$ are continuous across the layer, and so is h_3, according to eq. (6). Nevertheless $\Psi^\dagger\sigma_1\Psi$ and $\Psi^\dagger\sigma_2\Psi$ are discontinuous across the layer, and so is $\vec{h}_\parallel \equiv h_1\hat{x}_1 + h_2\hat{x}_2$, and, consequently, there is a superficial current density,

$$\vec{J}_s = -2c\mu_B\,\hat{x}_3\times\Psi^\dagger(0^+)\vec{\sigma}\Psi(0^+). \tag{12}$$

We next solve $\vec{\sigma}\cdot\vec{\nabla}\Psi = 0$ for a stack of layers under the simplifying assumption that all layers are identical:

$$\Psi = \sum_{\vec{k}\neq 0} c_{\vec{k}}\,\frac{e^{i\vec{k}\cdot\vec{x}}}{\sinh(kd/2)}\begin{pmatrix} \cosh\left[k\left(x_3 - d/2\right)\right] \\ i\frac{k_+}{k}\sinh\left[k\left(x_3 - d/2\right)\right] \end{pmatrix}. \tag{13}$$

The field $\vec{h}$ is obtained analytically by introducing eq. (13) into eq. (8) firstly, and next to eq. (6). There is a fundamental difference between *single* and *multiple* layer solutions described by eqs. (11) and (13), respectively. For a single layer $\langle\vec{h}\rangle = 0$, since $\langle\Psi^\dagger\vec{\sigma}\Psi\rangle = 0$. In fact for the single layer eq. (8) does not apply to determine $\vec{C}$. For a stack of layers $\langle\Psi^\dagger\sigma_3\Psi\rangle = \sum_{\vec{k}\neq 0}|c_{\vec{k}}|^2/\sinh^2(kd/2)$, and $\langle\Psi^\dagger\vec{\sigma}_\parallel\Psi\rangle = 0$. Thus the stack of layers behaves similarly to a solenoid, which renders $\langle h_3\rangle \geq 0$, and only $\langle\vec{h}_\parallel\rangle = 0$. The

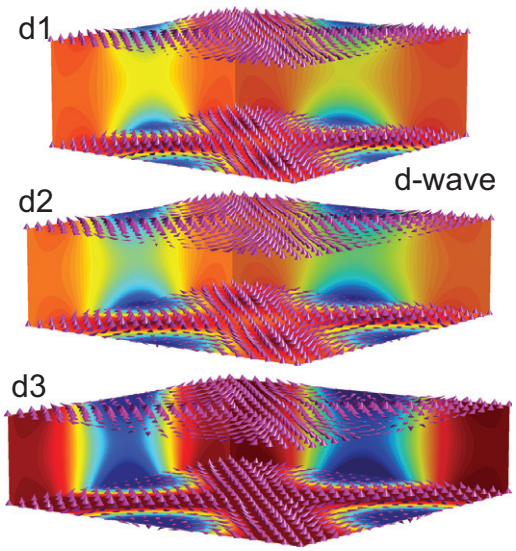

Fig. 3: (Color online) The d-wave local magnetic field component, perpendicular to the layers, h_3, is shown in colors (blue negative, green zero and red positive) at the walls of the dL^2 unit cell. The (cyan) cones depict the local magnetic field $\vec{h}$ infinitesimally *below* (top cones) and *above* (bottom cones) a layer.

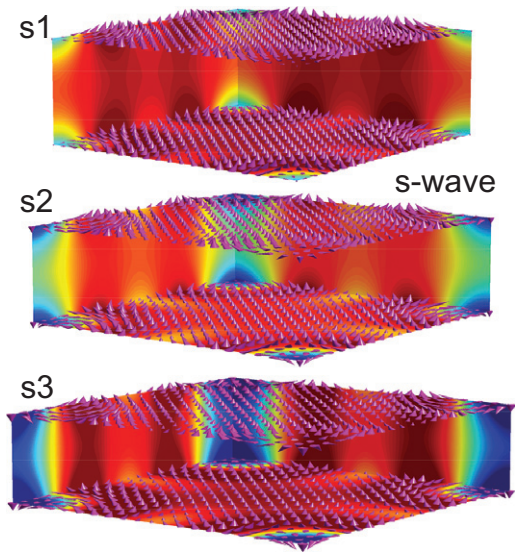

Fig. 4: (Color online) The s-wave local magnetic field component perpendicular to the layers, h_3, is shown in colors (blue negative, green zero and red positive) at the walls of the dL^2 unit cell. The (cyan) cones depict the local magnetic field $\vec{h}$ infinitesimally *below* (top cones) and *above* (bottom cones) the layer.

low component of eq. (13) vanishes in the middle plane ($x_3 = d/2$), and there $\Psi^\dagger \vec{\sigma}_\parallel \Psi|_{x_3=d/2} = 0$. Physically this means that $\vec{h}_\parallel$ has opposite signs in $0 < x_3 < d/2$ and $d/2 < x_3 < d$, and consequently there is a non-zero $\vec{J}_s$ in the layers. F_k and F_f are well defined only outside the layer, thus excluding $x_3 = 0$. The same holds for the multilayer solution of eq. (13), limited to $0 < x_3 < d$.

The gap density of the skyrmion state follows from eqs. (9) and (13), which give that

$$F_k = \frac{(h/d)^2}{\pi^2 m} \sum_{\vec{k}\neq 0} |c_{\vec{k}}|^2 \frac{kd/2}{\tanh(kd/2)}. \qquad (14)$$

The gap is not very sensitive to the small k regime as shown by the two limits of the function $f(z) = z/\tanh(z)$, $z \equiv kd/2$: $f(z \to 0) \to 1$, and $f(z = 1) \approx 1.3$. Nevertheless the region near to $z = 1$ matters, because, as shown below, there lives the skyrmion state, which is stable.

The d- and s-wave models. – Here we select the coefficients $c_{\vec{k}}$ in eq. (13) such that ψ_u has s or d angular momentum perpendicular to the layers, namely, ψ_u is an eigenvector of the operator $L_3 = (\hbar/i)(k_1\partial/\partial k_2 - k_2\partial/\partial k_1)$. We associate ψ_u to the superconducting state since the other component, ψ_d, breaks the time-reversal symmetry. The s and d states correspond to the eigenvalues $m = 0$ and $m = \pm 2$, respectively of $L_3 c_{\vec{k}} = \pm m\hbar c_{\vec{k}}$, $c_{\vec{k}} = (k_\pm)^m$. Therefore the s and d states correspond to $c^s_{\vec{k}} = \psi_0$ and $c^d_{\vec{k}} = \psi_0 \left(k_+^2 + k_-^2\right)/2k^2$, where ψ_0^2 is the density that determines h_{max} according to eq. (6). We choose $c_{\vec{k}}$ for the d-wave state to be an equal admixture of $m = 2$ and $m = -2$ states. Then they are eigenstates of L_3^2, and not of L_3. Although the coefficients $c^{d,s}_{\vec{k}}$ are common to both components of Ψ, ψ_d, is in a different L_3^2 state than ψ_u, because k_+ adds an extra angular momentum besides breaking the time reversal symmetry. For simplicity only the lowest fourier terms are included, and so, $\vec{k} = 2\pi\vec{n}/L$, $\vec{n} = n_1\hat{x}_1 + n_2\hat{x}_2$, where, $n_i = -1, 0, 1$, $i = 1, 2$. For the totally inhomogeneous state $n_1 = n_2 = 0$ is excluded.

The weak field $\vec{h}$ of the skyrmion state yields a negligible F_f, as compared to F_k, and consequently, the gap density of eq. (14) is the dominant term. The search of the optimal unit cell ratio, L/d, that minimizes F_f also determines the region of existence of the skyrmion state, which lives near this minimum. According to eq. (10) F_f plunges to a minimum within a small L range window, around $L/d \sim 3$ and 4 for d- and s-wave symmetries, respectively, as shown in fig. 2. The values d2 and s2 correspond to such minima while the other points (d1, d3) and (s1, s3) are arbitrary selections chosen below and above these minima. Figure 2 shows that the d-wave state (red curve, left scale) has almost ten times less stored magnetic energy than the s-wave state (black curve, right scale). Figures 3 and 4 show that the region around the center of the skyrmions are pockets of $h_3 < 0$, thus in opposite direction to the majority of the unit cell, which features $h_3 > 0$. The configurations of figs. 3 and 4 correspond to the three selected L/d ratios of fig. 2. The same red to blue scale applies to each of the three displayed cases. The (cyan) cones of figs. 3 and 4 depict $\vec{h}$ slightly below and above a layer, respectively. Because all layers are equivalent, the bottom plane of (cyan) cones shows $\vec{h}$ slightly above a layer.

Conversely, the top plane of (cyan) cones shows $\vec{h}$ slightly below a layer. In this way the cones around the center of the skyrmions clearly show the discontinuity of $\vec{h}_{\parallel}$, and so, the presence of $\vec{J}_s$ in the blue regions. Regions with a dominant h_3 component, have very weak $\vec{J}_s$, because h_3 is continuous across the layer. These regions take most of the unit cell, specially its center, where (cyan) cones point upward, but there is also the center of the skyrmions, where $h_3 < 0$. Notice that the configurations (d2, s2) contain more green color ($h_3 = 0$) than the (d1, s1), and (d3, s3) ones, respectively, in agreement to the fact that there the lowest magnetic energy is reached. Although (d3, s3) are the configurations with most intense fields (red, $h_3 > 0$; blue, $h_3 < 0$), their magnetic energies are larger than that of (d2, s2). The same holds for (d1, s1), which are the configurations with less $h_3 < 0$ regions as compared to the others.

We hope that the present macroscopic approach will bring some understanding to the microscopic mechanism of pairing in the underdoped regime of the cuprates [43].

Conclusion. – Using the first-order equations we show that the two-component order parameter layered superconductor has a topologically stable inhomogeneous state with a gap above the homogeneous ground state.

* * *

AAV-P and MMD acknowledge CNPq for financial support.

Note added in proofs: The Gnzburg-Landau equation can be solved by another approximate method, valid for $T = T^* = T_c$, that does not appeal to the integrated equation. The major results of this letters still hold under this method, which features $\vec{C} = 0$.

REFERENCES

[1] Schmalian J., *Mod. Phys. Lett. B*, **24** (2010) 2679.
[2] He R. H. *et al.*, *Science*, **331** (2011) 1579.
[3] Shekhter Arkady *et al.*, *Nature*, **498** (2013) 75.
[4] Alloul H., Ohno T. and Mendels P., *Phys. Rev. Lett.*, **63** (1989) 1700.
[5] Kaminski A. *et al.*, *Nature*, **416** (2002) 610.
[6] Xia J. *et al.*, *Phys. Rev. Lett.*, **100** (2008) 127002.
[7] Volovik G. E. and Gor'kov L. P., *Sov. Phys. JETP*, **61** (1985) 843.
[8] Varma C. M., *Phys. Rev. B*, **73** (2006) 155113.
[9] Fauqué B. *et al.*, *Phys. Rev. Lett.*, **96** (2006) 197001.
[10] Li Y. *et al.*, *Phys. Rev. B*, **84** (2011) 224508.
[11] Strässle S., Roos J., Mali M., Keller H. and Ohno T., *Phys. Rev. Lett.*, **101** (2008) 237001.
[12] Strässle S. *et al.*, *Phys. Rev. Lett.*, **106** (2011) 097003.
[13] MacDougall G. J. *et al.*, *Phys. Rev. Lett.*, **101** (2008) 017001.
[14] Sonier J. E. *et al.*, *Phys. Rev. Lett.*, **103** (2009) 167002.
[15] Tranquada J. M. *et al.*, *Phys. Rev. B*, **78** (2008) 174529.
[16] Li Jian-Xin, Wu Chang-Qin and Lee Dung-Hai, *Phys. Rev. B*, **74** (2006) 184515.
[17] Hoffman J. E. *et al.*, *Science*, **297** (2002) 1148.
[18] Vershinin M. *et al.*, *Phys. Rev. B*, **303** (2004) 1994.
[19] McElroy K. *et al.*, *Phys. Rev. Lett.*, **94** (2005) 197005.
[20] Islam Zahirul *et al.*, *Phys. Rev. Lett.*, **93** (2004) 157008.
[21] Rosen J. A. *et al.*, *Nat. Commun.*, **4** (2013) 1977.
[22] Batlogg B., *Phys. Today*, **44**, issue No. 6 (1991) 44.
[23] Abrikosov A. A., *Sov. Phys. JETP*, **5** (1957) 1174.
[24] Bogomolny E. B., *Sov. J. Nucl. Phys.*, **24** (1976) 449.
[25] Seiberg N. and Witten E., *Nucl. Phys. B*, **426** (1994) 19.
[26] Doria M. M., de C. Romaguera A. R. and Peeters F. M., *EPL*, **92** (2010) 17004.
[27] Vargas-Paredes A. A., Doria M. M. and Neto J. A. H., *J. Math. Phys.*, **54** (2013) 013101.
[28] Babaev Egor, Faddeev Ludvig D. and Niemi Antti J., *Phys. Rev. B*, **65** (2002) 100512.
[29] Skyrme T., *Nucl. Phys.*, **31** (1962) 556.
[30] Kälbermann G., Pari G. and Eisenberg J. M., *Phys. Rev. C*, **44** (1991) 899.
[31] Schmeller A. *et al.*, *Phys. Rev. Lett.*, **75** (1995) 4290.
[32] Volovik G. E. and Krusius M., *Physics*, **5** (2012) 130.
[33] Walmsley P. M. and Golov A. I., *Phys. Rev. Lett.*, **109** (2012) 215301.
[34] Raičević I. *et al.*, *Phys. Rev. Lett.*, **106** (2011) 227206.
[35] Yu X. Z. *et al.*, *Nature*, **465** (2010) 901.
[36] Pfleiderer C. *et al.*, *Nature*, **427** (2004) 227.
[37] Münzer W. *et al.*, *Phys. Rev. B*, **81** (2010) 041203.
[38] Vargas-Paredes Alfredo A. *et al.*, *J. Supercond. Nov. Magn.*, (2013) 1.
[39] Moshchalkov V. *et al.*, *Phys. Rev. Lett.*, **102** (2009) 117001.
[40] Sigrist M. and Ueda K., *Rev. Mod. Phys.*, **63** (1991) 239.
[41] Yanagisawa T. *et al.*, *J. Phys. Soc. Jpn.*, **81** (2012) 024712.
[42] Tinkham M., *Introduction to Superconductivity* (McGraw-Hill) 1996, p. 298.
[43] Marchetti P. A., Ye F., Su Z. B. and Yu L., *EPL*, **93** (2011) 57008.